Proceeding Paper

Crystal Structure of 2-(Ethoxymethylene)malononitrile and DFT Evaluation of the C-H···N≡C Close Contacts Energy [†]

Vyacheslav S. Grinev [1,2,*], Ilya A. Demeshko [1], Anna E. Sklyar [1] and Alevtina Yu. Yegorova [1]

[1] Institute of Chemistry, N.G. Chernyshevsky Saratov National Research State University, 83 Ulitsa Astrakhanskaya, 410012 Saratov, Russia; ilja.demeshko@yandex.ru (I.A.D.); annasklyar2502@gmail.com (A.E.S.); yegorovaay@gmail.com (A.Y.Y.)

[2] Institute of Biochemistry and Physiology of Plants and Microorganisms—Subdivision of the Federal State Budgetary Research Institution Saratov Federal Scientific Centre of the Russian Academy of Sciences (IBPPM RAS), 13 Prospekt Entuziastov, 410049 Saratov, Russia

[*] Correspondence: grinevvs@sgu.ru

[†] Presented at the 27th International Electronic Conference on Synthetic Organic Chemistry, 15–30 November 2023; Available online: https://ecsoc-27.sciforum.net/.

Abstract: 2-(Ethoxymethylene)malononitrile **1** is a very convenient building block for the construction of various heterocycles and it is assuming as an intermediate in different three-component reactions. Here we present the results of XRD of **1** demonstrating in crystal the linkage of the co-oriented molecules via C-H···N≡C non-covalent interactions. To evaluate the energy of such interactions, we conducted DFT simulations. The molecules of **1** are linked into infinite chains via C-H···N≡C close contacts with distance of 2.494 Å. When theoretical measuring the energy of H···N non-covalent interactions by DFT, it was determined by M06-2X functional equal to −1.20 kcal/mol meaning weak attraction.

Keywords: crystal structure; disorder; non-covalent interactions; quantum chemical modeling; interaction energy evaluating; 2-(ethoxymethylene)malononitrile

1. Introduction

As a part of our current study on functionalized analogs of azophenine, we recently synthesized 2-(ethoxymethylene)malononitrile (**1**) to clarify its crystal structure. This compound was reported for the first time in 1922 [1]. This simply built compound is a very convenient building block for the construction of various heterocycles [2,3] as well as for the introduction of the methane group into the nucleophile-containing structures leaving one or two nitrile groups intact for further transformations. Also, this compound is assumed as an intermediate in different three-component reactions [4]. There are in the literature a few mentions about the crystal structures of structurally related compounds with nitrile groups, namely, ethyl (E)-2-cyano-3-(thiophen-2-yl)acrylate [5], (*E*)-ethyl-2-cyano-3-(furan-2-yl)acrylate [6]. To the best of our knowledge, there is no information about the crystal structure of (1).

In this study, we present the results of X-ray diffraction of the titled compound, which demonstrates in crystal a discrete molecular disorder and the linkage of the co-oriented molecules via C-H···N≡C non-covalent interactions. To evaluate the energy of such interactions, we conducted DFT simulations.

2. Materials and Methods

2.1. Physical Measurements

The FTIR transmission spectrum was collected in a KBr pellet with FSM-1201 Fourier spectrometer (Infraspek, Russia) in the 4000–400 cm⁻¹ range. The ¹H (400 MHz) and

^{13}C NMR (100 MHz) spectra in acetone-d6 were recorded with a Varian (Agilent) 400 spectrometer (Agilent Technologies, Santa Clara, California, USA), internal standard was TMS. Chemical shifts (δ) are reported in ppm. Elemental analysis was performed on a CHNS analyzer "Elementar Vario MICRO cube" (Elementar Analysensysteme GmbH, Hanau, Germany). Melting point was determined on a Stuart™ SMP10 melting point apparatus (Cole-Parmer, Beacon Road, Stone, Staffordshire, ST15 0SA, UK). The progress of the reaction and the purity of the synthesized compound were monitored by TLC on ALUGRAM® SIL G UV254 plates (MACHEREY-NAGEL GmbH & Co. KG, Düren, Germany), a hexane-ethyl acetate-acetone (2:2:1) mixture was the eluent.

2.2. Synthesis, Characterization, and Crystallization

The 2-(ethoxymethylene)malononitrile (1) was obtained by the procedure described in [7] (Scheme 1).
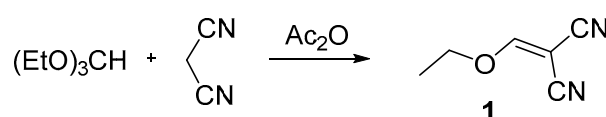
Scheme 1. Synthesis of the titled compound (**1**).

A mixture of 0.5 g (7.6 mmol) of malononitrile, 1.87 mL (11.4 mmol) of triethoxymethane, and 1.77 mL of acetic anhydride (18.9 mmol) were heated at 150 °C for 20 min in sealed vessels reactor (SVR) Monowave 50 (Anton Paar, Austria). After being cooled, the reaction mixture was concentrated under reduced pressure to a minimum volume. Formed crystals were separated, washed with cold ethanol, and dried in vacuo. A suitable single crystal was chosen for the XRD study. Yield 0.7 g (76%), mp 67.5–68.5 °C; FTIR, cm^{-1} 3443, 3212, 3033, 3006, 2944, 2905, 2434, 2228, 1956, 1887, 1763, 1611, 1552, 1472, 1449, 1397, 1373, 1317, 1259, 1219, 1154, 1107, 1009, 984, 883, 811, 792, 592, 542. The ^{1}H NMR (400 MHz, acetone) δ 8.25 (s, 1H), 4.55 (q, J = 7.2 Hz, 2H), 1.42 (t, J = 7.1 Hz, 3H). The ^{13}C NMR (100 MHz, acetone-d_6) δ 177.06, 112.50, 110.48, 75.07, 64.65, 14.49. Anal. calcd. for $C_6H_6N_2O$, %: C, 59.01; H, 4.95; N, 22.94; found: C, 59.08; H, 4.97; N, 22.96.

A suitable single crystal of 1 was obtained by slowly cooling its hot glacial acetic acid solution. The crystal was washed with cooled n-hexane and dried in vaccuo. The dimensions of the crystal were 0.55 × 0.40 × 0.35 mm^3.

2.3. Crystal Structure Determinations and Refinement

An X-ray diffraction study of (**1**) was performed an Xcalibur Ruby diffractometer (MoKα radiation, graphite monochromator, multi-scan) at 295 K. The empirical absorption correction was introduced by multi-scan method using SCALE3 ABSPACK algorithm [8]. The structure was solved with the olex2.solve program [9] and refined by the full-matrix least-squares method in the anisotropic approximation for all non-hydrogen atoms with the SHELXL program [10]. The hydrogen atoms were positioned geometrically and refined using a riding model with $U_{\text{iso}}(H) = 1.5U_{\text{eq}}(C)$ for methyl groups and $U_{\text{iso}}(H) = 1.2U_{\text{eq}}(C)$ for other moieties, and with C–H distances of 0.93 Å (CH), 0.96 Å (CH$_3$) or 0.97 Å (CH$_2$).

The crystal data, data collection, and structure refinement details are summarized in Table S1. The packing diagram and parameters of non-covalent interactions were obtained using Olex2 software [11].

2.4. DFT Calculations

All density functional theory calculations were carried out with the Gaussian 09 [12] program using high-performance computing cluster of National Research Saratov State University. Coordinates from X-ray data were used as initial and full geometry optimi-

zation of monomers and dimers (Figure 4) were performed B3LYP [13,14], CAM-B3LYP [15], M06-2X [16], MPWB95 [17], WB97XD [18], B97—D3 [19] functionals and the 6-311++G(*d*,*p*) basis set. The nature of stationary points found was confirmed by Hessian analysis by the absence of imaginary frequencies. The total energy gains were calculated as a difference between the energy of the dimer and doubled energy of the corresponding monomer (Table 1).

3. Results and Discussion

3.1. Crystal Structure Analysis

The content of the asymmetric unit of (**1**), along with the atom-labeling scheme, is shown on Figure 1. This structure has been deposited in the Cambridge Crystallographic Data Centre with deposition number CCDC 2180335. These data can be obtained free of charge via https://www.ccdc.cam.ac.uk/structures/ (or from the Cambridge Crystallographic Data Centre, 12, Union Road, Cambridge CB2 1EZ, UK; Fax: +44 1223 336033).
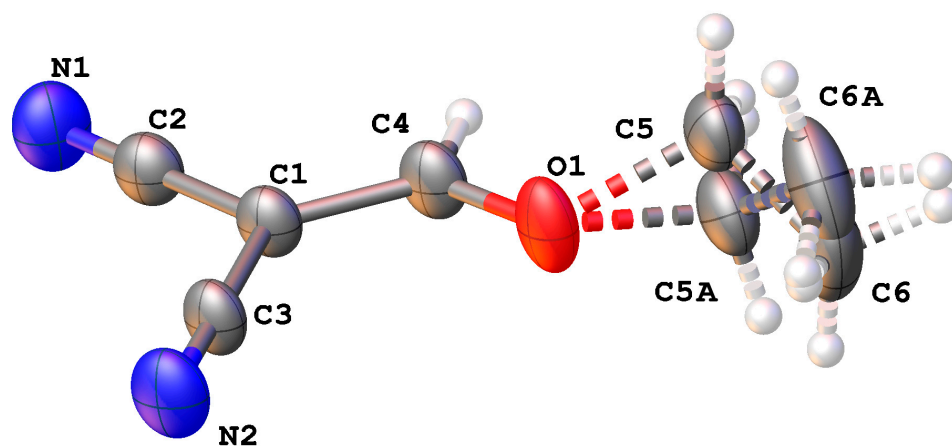

Figure 1. The geometry of (**1**) with atom labeling in the asymmetric unit. Disordered part is shown with dashed bonds. Displacement ellipsoids are drawn at the 50% probability level. Symmetry code used to generate equivalent atoms: (A) *x*, 1/2 − *y*, *z*.

Compound (**1**) crystallizes with *Z* = 2 in the monoclinic crystal system, space group *P* 2₁/*m*. The main part of the molecule of (**1**) demonstrates perfect planarity (atoms in (NC)2C=CH–O fragment lie in the same plane orthogonal to [010]) with RMSD of 0.000 Å except for the ethyl fragment. The C5-C6 atoms of the ethyl group present a discrete disorder due to the existence of two conformations of the ethyl moiety that overlay in the same crystallographic site. This disorder was modeled using two positions for the C5 and C6 atoms with equal occupancy values of 0.5 and total s.o.f. of 1.0. The split fragment is observed as a consequence of two ethyl moieties on the two opposite sides of the mirror plane that contains the main part of the molecule of (**1**). It is very similar to the crystal of ethyl (*E*)-2-cyano-3-(thiophen2-yl)acrylate, described by Castro Agudelo et al. [20].

3.2. Packing Features of (*1*)

The unit cell of (**1**) with a volume of 348.0 Å3 contains a pair of molecules oriented antiparallel to each other and parallel to the *a* axis (Figure 2). The package demonstrates C-H⋯N≡C close contacts with H⋯N distance of 2.494 Å giving infinite chains of co-oriented molecules parallel to the *a* axis and flat-parallel layers coplanar to the *ac* plane. Also, there are weak (Et)H⋯N≡C in plane close contacts of 2.855 Å.
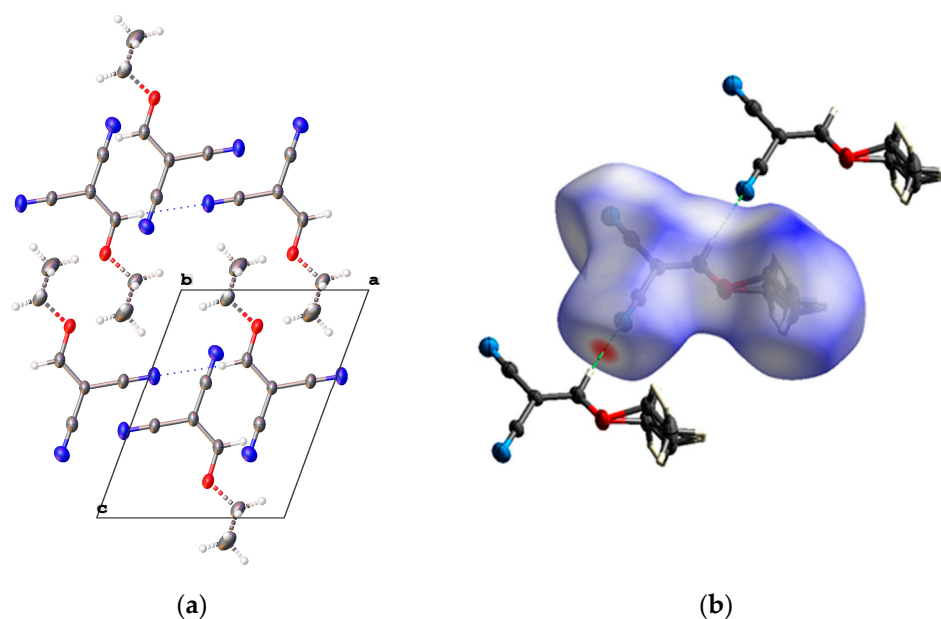
(**a**)   (**b**)

Figure 2. Extended packing diagram of molecules of (**1**), showing close C-H⋯N≡C contacts (blue dots). Dashed bonds show a disorder of ethyl groups (**a**). Hirshfeld surface diagram with a fragment of the extended packaging diagram of molecules of (**1**) showing non-covalent close contacts (**b**).

In crystal, there are two intermolecular interplanar hydrogen bonds between molecules of neighboring layers. The O⋯H contacts are between oxygen atom of the molecule and hydrogen atoms of CH_2 and CH_3 groups in the disordered ethyl group of the molecule of neighboring layers. The geometric parameters of hydrogen bonds are presented in Table 1.

Table 1. Geometric parameters of the intermolecular hydrogen bonds in the crystal of **1**.

Moiety	H⋯O, Å	D⋯A, Å	D−H⋯A, °
CH_2	3.294	3.424	126.5
CH_3	2.761	3.949	127.0

3.3. Hirshfeld Surface Analysis

Hirshfeld surface analysis [21] of the studied crystal allows us to visualize intermolecular interactions to prove the presence of weakly pronounced contacts. The Hirshfeld surface diagram, dnorm, with transparency (Figure 2b), indicates (in red) locations of the strongest intermolecular contacts.

The N⋯H/H⋯N contacts with the portion of 43.5% of all contacts in the crystal of 1 demonstrate their significance for the stabilization of the lattice. The O⋯H/H⋯O contacts, mostly, are represented by intermolecular weak hydrogen bonds of the oxygen atom of one molecule and protons of the ethyl moiety of the neighboring molecule. The portion of such contacts are of 8.3%. The contribution of the H⋯H intermolecular interactions in crystals 1 amount to only 17.6% and reflecting a repulsion of protons of ethyl groups.

In crystal of **1**, the molecules in the package are connected to each other by intermolecular intra- (weak (Et)H⋯N≡C in plane close contacts) and interplanar (O⋯H(Et) contacts) non-covalent interactions including hydrogen-bond-like C-H⋯N≡C contacts prevailing over the repulsive forces of H⋯H contacts between hydrogen atoms in ethyl groups.

3.4. Theoretical Evaluation of the Close Contact Energy

For evaluation of the energetics of close contacts in crystals of (1), DFT calculations were performed on the monomers and dimers. The models of monomers and dimers were built using coordinates from X-ray data (Figure 3).
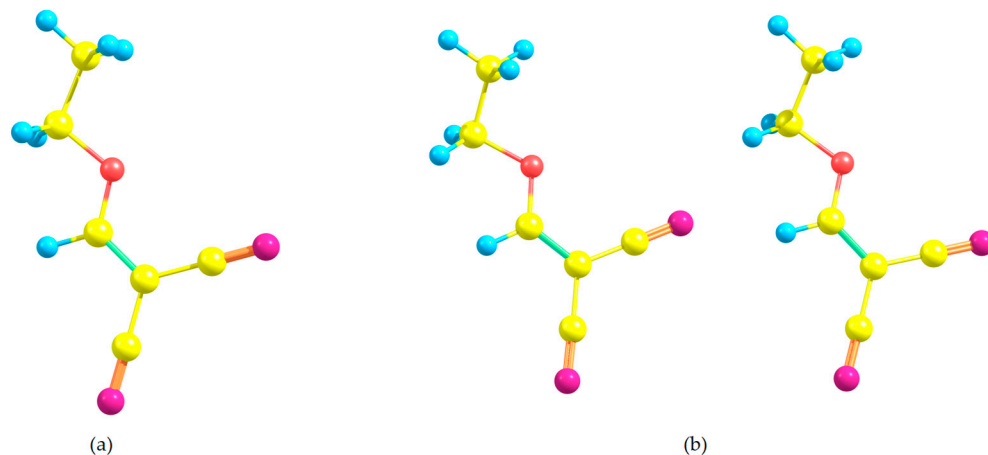

Figure 3. A diagram showing the models used in calculation of the energy of C-H···N≡C close contacts in crystals of (1); (**a**) monomer, (**b**) dimer.

The choice of the appropriate functional in DFT is crucial for better prediction accuracy. Many popular hybrid functionals like B3LYP describe more accurately the geometry of the single molecule but are almost useless in the modeling systems consisting of molecules connected by non-covalent interactions. Besides, the dimer as the system of a pair of identical molecules with two strongly pronounced hydrogen bonds is relatively simple for modeling even by functionals, which have no dispersion corrections. So, we have chosen some functionals, namely, B3LYP, CAM-B3LYP, M06-2X, MPWB95, WB97XD, and B97-D3 used frequently for modeling non-covalent interacted systems with the 6-311++G(*d*,*p*) basis set. A criterion of the accurate prediction of the model was the reproduction of geometry of the close contacts as well as the general disposition of molecules in contrast to X-ray data. Obtained results are summarized in Table 2.

Table 2. Geometric parameters of the close contacts and the calculated energy.

Method	H···N, Å	D···A, Å	D—H···A, °	E (kcal/mol)
XRD	**2.494**	**3.423**	**176.22**	-
M06-2X	**2.424**	**3.472**	**176.23**	-1.20
MPWB95	2.561	3.611	160.52	-0.36
B97-D3	2.423	3.483	163.65	-1.27
WB97XD	2.385	3.439	162.61	-1.53

All the functionals used gave very similar results describing the geometry of monomers and dimers of (**1**), except for the B3LYP and CAM-B3LYP methods, which returned abnormally huge energy values (not shown in Table 3). The M06-2X functional gave the closest values of geometric data in contrast to all applied functionals. It allows us to consider the energy calculated by the M06-2X functional as the closest to the experimental one. Other functionals have given energies, either overestimated or underestimated, which can lead to distorted energy values. The obtained energy value of -1.20 kcal/mol confirms that in the crystal of compound (**1**), the connection between the molecules occurs due to H···N non-covalent interactions, which may be defined as weak hydrogen bonds.

4. Conclusions

The unit cell of the single crystal of compound (1), which is a relatively simple non-cyclic organic compound, consists of "head to tail" ordered molecules. Ethyl substituent demonstrates a disorder with equal occupancy values of 0.5. The molecules of (1) are linked into infinite chains of co-oriented molecules parallel to the *a* axis via C-H···N≡C close contacts with a distance of 2.494 Å. When theoretical measuring the energy of H···N non-covalent interactions by DFT, it was determined that the M06-2X functional most accurately determined the energy of the non-covalent intermolecular bond, which is equal to −1.20 kcal/mol. According to the energy value magnitude, one can state that the interaction is a weak hydrogen bond. There are also weak interplanar intermolecular hydrogen bonds >O···H- between oxygen atom and the ethyl moiety.

Supplementary Materials: The following supporting information can be downloaded at: www.mdpi.com/xxx/s1, Table S1: Experimental details of the X-ray diffraction analysis;.

Author Contributions: Conceptualization, V.S.G.; methodology, V.S.G. and A.Y.Y.; software, V.S.G.; validation, V.S.G., I.A.D., A.E.S., A.Y.Y.; formal analysis, I.A.D. and A.E.S.; investigation, I.A.D. and A.E.S.; resources, V.S.G. and A.Y.Y.; writing—original draft preparation, V.S.G and I.A.D.; writing—review and editing, A.E.S.; supervision, V.S.G. and A.Y.Y. All authors have read and agreed to the published version of the manuscript.

Institutional Review Board Statement: Not applicable.

Informed Consent Statement: Not applicable.

Data Availability Statement: Data available on request.

Conflicts of Interest: The authors declare no conflict of interest.

References

1. Diels, O.; Gärtner, H.; Kaack, R. Über Versuche zur Darstellung des Carbonylcyanids und eine Methode zur Gewinnung ungesättigter Amino-Säuren. *Berichte Der Dtsch. Chem. Ges. (A B Ser.)* **1922**, *55*, 3439–3448. https://doi.org/10.1002/cber.19220551013.
2. Ochiai, M.; Yamamoto, S.; Suefuji, T.; Chen, D. Stereoselective synthesis of (*Z*)-enethiols and their derivatives: Vinylic SN2 reaction of (*E*)-alkenyl (phenyl)-*λ*3-iodanes with thioamides. *Org. Lett.* **2001**, *3*, 2753–2756. https://doi.org/10.1021/ol016356c.
3. Konakahara, T.; Sugama, N.; Yamada, A.; Kakehi, A.; Sakai, N. Cyclization reaction of N-silyl-1-azaallyl anions with Michael acceptors as a new synthetic method of 2,3,5,6-tetra- and 2,3,6-trisubstituted pyridines. *Heterocycles* **2001**, *55*, 313–322. https://doi.org/10.3987/COM-00-9096.
4. Osipov, A.K.; Anis'kov A. A.; Yegorova, A.Y. Synthesis and configuration of (arylamino) methylidene-3*H*-furan-2-ones. *Russ. J. Org. Chem.* **2017**, *53*, 210–214. https://doi.org/10.1134/S1070428017020117.
5. Al-Refai, M.; Ali, B.F.; Said, A.B.; Geyer, A.; Marsch, M.; Harms, K. Synthesis, characterization, crystal structure and supramolecularity of ethyl (*E*)-2-cyano-3-(3-methylthiophen-2-yl) acrylate and a new polymorph of ethyl (*E*)-2-cyano-3-(thiophen-2-yl) acrylate. *Acta Crystallogr. Sect. E: Crystallogr. Commun.* **2019**, *75*, 1357–1361. https://doi.org/10.1107/S2056989019011435.
6. Kalkhambkar, R.G.; Gayathri, D.; Gupta, V.K.; Kant, R.; Jeong, Y.T. (*E*)-Ethyl 2-cyano-3-(furan-2-yl) acrylate. *Acta Crystallogr. Sect. E: Struct. Rep. Online* **2012**, *68*, 1482. https://doi.org/10.1107/S1600536812016510.
7. Ding, R.; He, Y.; Xu, J.; Liu, H.; Wang, X.; Feng, M.; Qi, C.; Zhang, J.; Peng, C. Preparation and bioevaluation of 99mTc nitrido radiopharmaceuticals with pyrazolo [1,5-a]pyrimidine as tumor imaging agents. *Med. Chem. Res.* **2012**, *21*, 523–530. https://doi.org/10.1007/s00044-011-9558-8.
8. CrysAlisPro, Agilent Technologies, Version 1.171.37.33 (release 27-03-2014 CrysAlis171 .NET).
9. Bourhis, L.J.; Dolomanov, O.V.; Gildea, R.J.; Howard, J.A.K.; Puschmann, H.J. *Appl. Crystallogr.* **2009**, *42*, 339. https://doi.org/10.1107/S2053273314022207.
10. Scheldrick, G.M. SHELXT-Integrated space-group and crystals-structure determination. *Acta Crystallogr. Sect. A Found. Adv.* **2015**, *71*, 3–8. https://doi.org/10.1107/S2053273314026370.
11. Dolomanov, O.V.; Bourhis, L.J.; Gildea, R.J.; Howard, J.A.K.; Puschmann, H.J. *Appl. Cryst.* **2009**, *42*, 339. https://doi.org/10.1107/S0021889808042726.

12. Frisch, M.; Trucks, G.; Schlegel, H.; Scuseria, G.; Robb, M.; Cheeseman, J.; Scalmani, G.; Barone, V.; Mennucci, B.; Petersson, G.; et al. *Gaussian 09, Rev. C.01*; Gaussian, Inc.: Wallingford, CT, USA, 2010.

13. Becke, A.D. Density-functional exchange-energy approximation with correct asymptotic behavior. *Phys. Rev. A* **1998**, *38*, 3098–3100. https://doi.org/10.1103/PhysRevA.38.3098.

14. Lee, C.; Yang, W.; Parr, R.G. Development of the Colle-Salvetti correlation-energy formula into a functional of the electron density. *Phys. Rev. B* **1988**, *37*, 785–789. https://doi.org/10.1103/PhysRevB.37.785.

15. Yanai, T.; Tew, D.P.; Handy, N.C. A new hybrid exchange–correlation functional using the Coulomb-attenuating method (CAM-B3LYP). *Chem. Phys. Lett.* **2004**, *393*, 51–57. https://doi.org/10.1016/j.cplett.2004.06.011.

16. Zhao, Y.; Truhlar, D.G. The M06 suite of density functionals for main group thermochemistry, thermochemical kinetics, non-covalent interactions, excited states, and transition elements: Two new functionals and systematic testing of four M06-class functionals and 12 other functionals. *Theor. Chem. Acc*. **2008**, *120*, 215–241. https://doi.org/10.1007/s00214-007-0310-x.

17. Zhao, Y.; Truhlar, D.G. Hybrid Meta Density Functional Theory Methods for Thermochemistry, Thermochemical Kinetics, and Noncovalent Interactions: The MPW1B95 and MPWB1K Models and Comparative Assessments for Hydrogen Bonding and van der Waals Interactions. *J. Phys. Chem*. **2004**, *108*, 6908–6918. https://doi.org/10.1021/jp048147q.

18. Remya, K.; Suresh, C.H. Which density functional is close to CCSD accuracy to describe geometry and interaction energy of small noncovalent dimers? A benchmark study using Gaussian09. *J. Comput. Chem*. **2013**, *34*, 1341–1353. https://doi.org/10.1002/jcc.23263.

19. Grimme, S. Semiempirical GGA-type density functional constructed with a long-range dispersion correction *J. Comput. Chem*. **2006**, *27*, 1787–1799. https://doi.org/10.1002/jcc.20495.

20. Castro Agudelo, B.; Cárdenas, J.C.; Macías, M.A.; Ochoa-Puentes, C.; Sierra, C.A. Crystal structure of ethyl (*E*)-2-cyano-3-(thiophen-2-yl) acrylate: Two conformers forming a discrete disorder. *Acta Crystallogr. Sect. E: Crystallogr. Commun.* **2017**, *73*, 1287–1289. https://doi.org/10.1107/S2056989017010799.

21. Hirshfeld, H.L. Bonded-atom fragments for describing molecular charge denseties. *Theor. Chim. Acta* **1977**, *44*, 129–138. https://doi.org/10.1007/BF00549096.